The greater curvature in *mdr1* seedlings could have resulted from a longer period of differential growth or from a steeper growth differential being in effect for a similar period of time. A kinetic analysis of curvature development based on electronic image analysis showed that the latter was true. The hypocotyl angle of wild-type and *mdr1* seedlings was monitored at 15-min intervals after gravitational stimulation (Fig. 3a). A plot of the first derivative of the time series shows the rate of curvature development over time (Fig. 3b) and establishes that *mdr1* hypocotyls curved approximately twice as fast but over the same time course as those of the wild type. Thus, the greater curvature of the *mdr1* hypocotyl was due to a steeper growth differential across the stem, not a more persistent one with the same magnitude as that of the wild type. It would follow, according to the Cholodny–Went theory of tropisms[11], that a larger transverse auxin gradient developed in the mutant during this 2-h period. Mislocalized PIN1, together with PIN3 in its normal position along lateral walls[12], could enable greater radial auxin flux, leading to the steeper, although transient, auxin concentration gradient inferred from the kinetics of gravitropic curvature development.

Phototropism, another curvature response driven by a transverse auxin concentration gradient[11,12], was about 30% greater in *mdr1* seedlings than in the wild type after 90 min of unilateral blue light. Figure 3c shows data obtained with the *mdr1-1* allele, and Fig. 3d shows that *mdr1-2* seedlings responded very similarly. The enhancement of both gravitropism and phototropism supports the conclusion that MDR1 functions in the growth-control phase of tropisms, as opposed to the stimulus-sensing phase. The initial phase of the phototropic response was not quickened by the *mdr1* mutation to the same extent as the gravitropic response, possibly because *MDR1* expression is decreased by the phototropic light stimulus or because the PIN1 localization phenotype was less severe in light-grown *mdr1* hypocotyls (Fig. 1). Future studies will examine whether other *MDR* family members also influence the distribution of PIN1, whether the interaction is direct or is a result of changes in polarity maintained by auxin gradients, and whether there are specific relationships between particular members of the MDR and PIN families of membrane transport proteins. □

Methods

Plant material

The wild type used in all experiments was the WS ecotype of *Arabidopsis thaliana*. MDR1 and PGP1 refer to the loci identified as At3g28860 and At2g36910, respectively. Images were captured with a SPOT camera and processed using Adobe Photoshop 5.0.

Immunolocalization

Arabidopsis seedlings were grown without sucrose on 1% phytagar plates, 1/4 Murashige and Skoog basal salts, pH 4.85, at 22 °C, under illumination (100 μmol $m^{-2} s^{-1}$) for 14 h a day for light-grown seedlings or in complete darkness. Five days after planting, seedlings were prepared for immunolocalization as described previously[13] with the following changes: seedlings were digested for 90 min in 0.5% pectolyase, 20% Triton X-100; Triton X-100 was omitted from the washes. Affinity-purified anti-PIN1 antibody[10] was diluted 1:400. Affinity-purified anti-AHA2 antibody was diluted 1:300. The secondary antibody was Alexa Fluor 488 conjugate (Molecular Probes, Eugene, Oregon) diluted 1:400. Immunofluorescence imaging was performed with an epifluorescence microscope (Eclipse E 800; Nikon, Melville, New York) equipped with a 450–490-nm excitation filter (model number 41017, Chroma Technology Corporation, Brattleboro, Vermont), a 495-nm dichroic mirror and a 500–530-nm emission barrier pass filter (Chroma), or with a confocal laser scanning microscope (Eclipse 800; Nikon) equipped with an argon laser (488 nm) (Bio-Rad). Green HeNe laser (543 nm, 1.4 mW) and a red laser diode (638 nm, 5 mW) were used for autofluorescence detection. Images were captured with a SPOT camera and processed using Adobe Photoshop 5.0.

Quantifying tropisms

All mutants and double mutants were isolated and constructed as described previously[5]. Seedlings were grown on minimal salt medium (1 mM $CaCl_2$, 1 mM KCl, 1% agar). To measure hypocotyl gravitropism, seedlings were grown along the surface of vertical agar plates in light for 1 day, then transferred to darkness for 1.5 days before the plates were reoriented by 90°. The angle made by the hypocotyl apex relative to the original gravity vector was determined from digital images acquired at 15-min intervals after reorientation for the time-course description or after 18 h of gravitational stimulation to determine the final steady-state angle. For phototropism, the seedlings were allowed to grow in darkness for 2 h before the vertical plate was illuminated from the side with blue light (0.07 μmol $m^{-2} s^{-1}$) produced by a bank of light-emitting diodes (described previously[14]) and passed through a slit before reaching the seedlings. Images of seedlings were recorded, every 10 min after the onset of unilateral irradiation, with a previously described imaging apparatus[14]. The angle of curvature was measured from the digital images at selected time points after the response became detectable.

Received 15 January; accepted 28 April 2003; doi:10.1038/nature01716.

1. Muday, G. K. & DeLong, A. Polar auxin transport: controlling where and how much. *Trends Plant Sci.* **6,** 535–542 (2001).
2. Gil, P. *et al.* BIG: a calossin-like protein required for polar auxin transport in *Arabidopsis*. *Genes Dev.* **15,** 1985–1997 (2001).
3. Friml, J. & Palme, K. Polar auxin transport—old questions and new concepts? *Plant Mol. Biol.* **49,** 273–284 (2002).
4. Ambudkar, S. V. *et al.* Biochemical, cellular, and pharmacological aspects of the multidrug transporter. *Annu. Rev. Pharmacol. Toxicol.* **39,** 361–398 (1999).
5. Noh, B., Murphy, A. S. & Spalding, E. P. Multidrug resistance-like genes of *Arabidopsis* required for auxin transport and auxin-mediated development. *Plant Cell* **13,** 2441–2454 (2001).
6. Sánchez-Fernández, R., Davies, T. G. E., Coleman, J. O. D. & Rea, P. A. The *Arabidopsis thaliana* ABC protein superfamily, a complete inventory. *J. Biol. Chem.* **276,** 30231–30244 (2001).
7. Murphy, A. S., Hoogner, K. R., Peer, W. A. & Taiz, L. Identification, purification, and molecular cloning of *N*-1-naphthylphthalamic acid-binding plasma membrane-associated aminopeptidases from *Arabidopsis*. *Plant Physiol.* **128,** 935–950 (2002).
8. Sidler, M., Hassa, P., Hasan, S., Ringli, C. & Dudler, R. Involvement of an ABC transporter in a developmental pathway regulating hypocotyl cell elongation in the light. *Plant Cell* **10,** 1623–1636 (1998).
9. Geldner, N., Friml, J., Stierhof, Y.-D., Jürgens, G. & Palme, K. Auxin transport inhibitors block PIN1 cycling and vesicle trafficking. *Nature* **413,** 425–428 (2001).
10. Gälweiler, L. *et al.* Regulation of polar auxin transport by AtPIN1 in *Arabidopsis* vascular tissue. *Science* **282,** 2226–2230 (1998).
11. Muday, G. K. Auxins and tropisms. *J. Plant Growth Regul.* **20,** 226–243 (2001).
12. Friml, J., Wisniewska, J., Benková, E., Mendgen, K. & Palme, K. Lateral redistribution of auxin efflux regulator PIN3 mediates tropism in *Arabidopsis*. *Nature* **415,** 806–809 (2002).
13. Harper, J. D. I. *et al.* A simple and rapid technique for the immunofluorescence confocal microscopy of intact *Arabidopsis* root tips: Localization of a centrin-like protein to higher plant plasmodesmata. *Cytobios* **87,** 71–78 (1996).
14. Folta, K. M. & Spalding, E. P. Unexpected roles for cryptochrome 2 and phototropin revealed by high-resolution analysis of blue light-mediated hypocotyl growth inhibition. *Plant J.* **26,** 471–478 (2001).

Supplementary Information accompanies the paper on **www.nature.com/nature**.

Acknowledgements We thank K. Palme for the PIN1 antibody, M. Sussman and S. Bednarek for the AHA2 antibody, and J. Wagner for technical assistance.

Competing interests statement The authors declare that they have no competing financial interests.

Correspondence and requests for materials should be addressed to E.P.S. (spalding@wisc.edu).

Chromosome cohesion is regulated by a clock gene paralogue TIM-1

Raymond C. Chan*, Annette Chan*, Mili Jeon†, Tammy F. Wu*, Danielle Pasqualone*, Ann E. Rougvie‡ & Barbara J. Meyer*

* *Howard Hughes Medical Institute and Department of Molecular and Cell Biology, University of California, Berkeley, California 94720-3204, USA*
† *Department of Biochemistry, University of Minnesota, St Paul, Minnesota 55108, USA*
‡ *Department of Genetics, Cell Biology and Development, University of Minnesota, Minneapolis, Minnesota 55455, USA*

Faithful transmission of the genome requires that a protein complex called cohesin establishes and maintains the regulated linkage between replicated chromosomes before their segregation[1,2]. Here we report the unforeseen participation of *Caenorhabditis elegans* TIM-1, a paralogue of the *Drosophila* clock protein TIMELESS, in the regulation of chromosome cohesion. Our biochemical experiments defined the *C. elegans* cohesin complex and revealed its physical association with TIM-1. Functional relevance of the interaction was demonstrated by aberrant

mitotic chromosome behaviour, embryonic lethality and defective meiotic chromosome cohesion caused by the disruption of either TIM-1 or cohesin. TIM-1 depletion prevented the assembly of non-SMC (structural maintenance of chromosome) cohesin subunits onto meiotic chromosomes; however, unexpectedly, a partial cohesin complex composed of SMC components still loaded. Further disruption of cohesin activity in meiosis by the simultaneous depletion of TIM-1 and an SMC subunit decreased homologous chromosome pairing before synapsis, revealing a new role for cohesin in metazoans. On the basis of comparisons between TIMELESS homologues in worms, flies and mice, we propose that chromosome cohesion, rather than circadian clock regulation, is the ancient and conserved function for TIMELESS-like proteins.

Cohesin contains two SMC subunits, Smc1 and Smc3, and two non-SMC subunits, Scc1 (Mcd1/Rad21) and Scc3 (stromal antigen/Psc3)[1,2]. Cohesin is loaded onto chromosomes before S phase and establishes cohesion between the duplicated chromosomes (sister chromatids) during DNA replication[1,2]. This regulated linkage is released in preparation for chromosome segregation through a well-defined mechanism that involves the phosphorylation and proteolytic cleavage of the non-SMC cohesin subunit Scc1 (refs 3, 4). By contrast, the mechanisms that underlie the loading and assembly of cohesin onto chromosomes are poorly understood.

To analyse the regulation of chromosome cohesion in *C. elegans*, we first identified homologues of conserved cohesin subunits. Single candidates for Smc1 (open reading frame (ORF) F28B3.7), Smc3 (ORF Y47D3A.26) and Scc3 (ORF F18E2.3) were found in the *C. elegans* genome database. We showed that *him-1* (high incidence of males)[5] encodes SMC-1 (see Methods), and *him-1* mutations cause chromosome segregation defects expected for a mutation in a cohesin subunit (see below and ref. 6). Of three candidates[7] with similarity to cohesin subunit Scc1/Mcd1, COH-2 (ORF F10G7.4) is the true orthologue (see below), prompting us to rename it SCC-1.

True cohesin components in *C. elegans* should assemble into a complex, like those of other organisms. Anti-SMC-1 antibodies precipitated SMC-3, SCC-3 and SCC-1 from embryonic extracts (Fig. 1a). Three controls demonstrated specificity for the co-immunoprecipitation. First, western blots of a mock immunoprecipitation control detected none of the proteins (Fig. 1a). Second, SMC-1 antibodies failed to precipitate two X-chromosome-bound SMC dosage compensation proteins, DPY-27 and MIX-1 (refs 8, 9; Fig. 1a). Last, antibodies against MIX-1, also a condensin complex subunit that assembles onto mitotic chromosomes, failed to precipitate cohesin (Fig. 1a). Reciprocal co-immunoprecipitation of SMC-1, SMC-3 and SCC-3 with anti-SCC-1 antibodies confirmed the formation of a stable cohesin complex (Fig. 1b).

Using a biochemical approach, we sought other components essential for chromosome cohesion. Unique protein bands from SMC-1 immunoprecipitations were identified (Fig. 1c) and analysed by mass spectrometry (Supplementary Table 1). As expected, SMC-1 and SMC-3 were among the proteins in the bands at relative

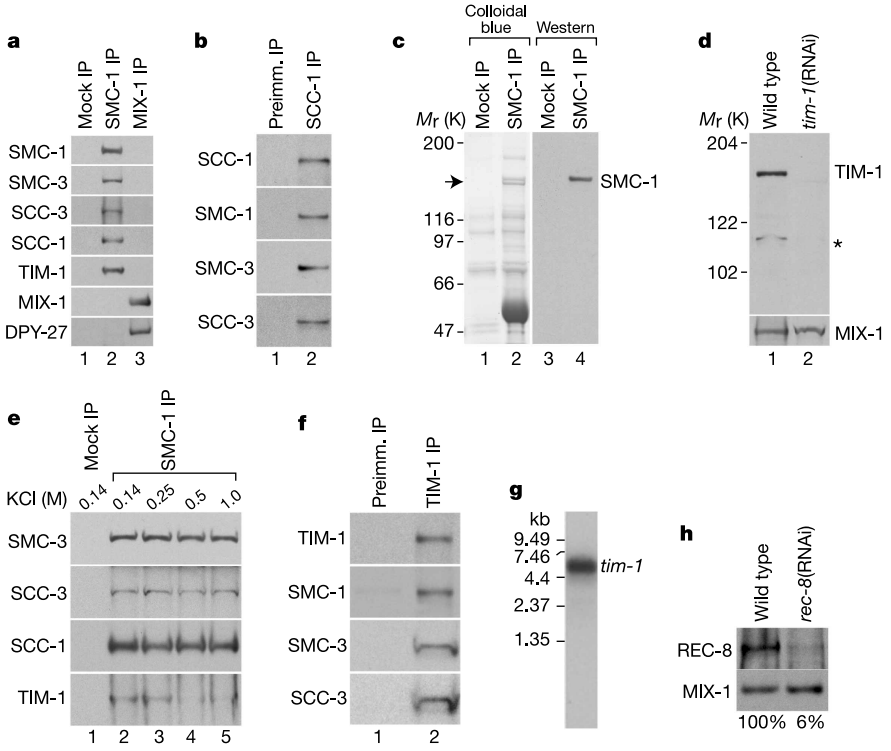

Figure 1 *C. elegans* TIM-1, a paralogue of the circadian clock protein TIMELESS, associates with the cohesin complex. **a**–**f**, **h**, Western blots. **a**, **b**, **e**, Immunoprecipitation (IP) reactions with antibodies against SMC-1 (**a**, **e**) or SCC-1 (**b**) co-precipitated the four cohesin subunits from embryonic extracts, indicating the formation of a stable complex. **c**, Cohesin-associated protein bands (arrow), similar in mobility to SMC-1 (M_r 150K), were identified by comparison of mock and SMC-1 immunoprecipitations stained with colloidal blue. Peptide mass fingerprinting showed that the bands included SMC-1, SMC-3 and TIM-1 (Supplementary Table 1). The M_r 180K band includes vitellogenin, a common contaminant in embryonic extracts. **d**, Antibodies against TIM-1 specifically recognized full-length (M_r 150K) TIM-1 and a post-lysis cleavage product of M_r 120K (asterisk) from whole worm lysates; both proteins, but not MIX-1, were depleted by *tim-1* RNAi. **a**, **e**, SMC-1 immunoprecipitation enriched for TIM-1, but its association with the cohesin complex was more salt-sensitive (it dissociated at 0.5 M KCl or more) than core cohesin subunits (**e**). **f**, Reciprocal TIM-1 immunoprecipitation confirmed the cohesin interaction. **g**, Northern blots with a genomic DNA probe spanning exons 6 and 7 detected a single 5.5-kb *tim-1* mRNA transcript. **h**, Estimate of REC-8 protein concentrations in *rec-8*(RNAi) animals; the values below the gels are REC-8 concentrations normalized to MIX-1 and compared to relative to wild-type animals.

molecular mass 150,000 (M_r 150K). In addition, a significant number of peptide fragments matched the tryptic peptides predicted for worm ORF Y75B8A.22, which was originally named *tim-1* (ref. 10) on the basis of its similarity to *Drosophila timeless*, a regulator of circadian rhythm.

Using TIM-1-specific antibodies (Fig. 1d and Methods) we confirmed the association of TIM-1 with cohesin. Both SMC-1 and SCC-1 immunoprecipitations were specifically enriched in TIM-1 (Fig. 1a, e, and data not shown). The reciprocal TIM-1 immunoprecipitation precipitated SMC-1, SMC-3 and SCC-3 (Fig. 1f). More stringent wash conditions (at least 0.5 M KCl) dissociated some TIM-1 from the cohesin complex, but the precipitated core cohesin complex was stable at 1 M KCl without TIM-1 (Fig. 1e). Thus, TIM-1 associates specifically with cohesin but is less tightly connected than other subunits.

The connection between TIM-1 and cohesin was unexpected, given the function of *Drosophila timeless* in the perpetuation and entrainment of circadian rhythm through its interaction with the clock gene *period* (*per*)[11,12]. However, several recent discoveries hinted that *timeless* homologues have an essential function that is independent of circadian rhythm regulation. *Drosophila* has a *timeless* paralogue called *timeout*, which more strongly resembles the single *C. elegans* and mammalian homologues than does *timeless*[13,14]. The function of *Drosophila timeout* is unknown, but knockout of the mouse m*Tim1* gene causes early embryonic lethality[14], whereas *timeless* mutant flies are fully viable. Finally, cryptochromes (mCry1/2) fulfil functions in mammalian circadian rhythm provided by TIMELESS in flies[12]. The connection between *C. elegans* TIM-1 and cohesin provides a clue to the likely ancient and conserved role for *timeless*/*timeout* homologues in metazoans.

To assess the function of TIM-1 *in vivo*, we first examined whether TIM-1 depletion affected *C. elegans* viability and chromosome segregation. TIM-1 and cohesin have similar cell-cycle-dependent patterns of subcellular localization during mitosis in somatic and germline tissues (Supplementary Fig. 1b). At interphase, TIM-1 and cohesin subunits accumulate most intensely and have a diffuse nuclear appearance. By the metaphase–anaphase transition, concentrations of both are greatly diminished and the proteins seem to be excluded from the compacted DNA. The disruption of either *tim-1* or individual cohesin genes by RNA-mediated interference (RNAi) caused complete embryonic lethality (Supplementary Table 2). Most nuclei of dying embryos had two 5S ribosomal DNA (rDNA) fluorescence *in situ* hybridization (FISH) signals (Fig. 2a), indicating normal chromosome segregation. Occasional nuclei had more than two FISH signals, perhaps from the premature dissociation of sister chromatids (Fig. 2a). However, nuclei from embryos treated with double RNAi against *him-1* and either *scc-1* or *tim-1* had numerous FISH signals, indicating severe chromosome segregation defects and extensive aneuploidy (Fig. 2a). By comparison, RNAi to *tim-1* only (Fig. 2b) caused aberrant chromosome segregation during germline mitosis that resembled the defective segregation in *him-1(h55)* (Fig. 2b) or *him-1(h134)* (Supplementary Fig. 1a, c) null mutants (see Methods). These results suggest a role for TIM-1 and other *timeless* paralogues in the establishment and/or maintenance of sister-chromatid cohesion in metazoans.

The role of TIM-1 in chromosome cohesion can be resolved further by analysing *tim-1* mutant defects in meiosis, where cohesion and other cohesin-dependent functions are essential for homologous chromosome synapsis, recombination and segregation[15]. We show below that TIM-1 has an essential function in meiotic chromosome cohesion by means of its regulation of cohesin subunits.

A description of wild-type meiotic chromosome behaviour provides the context for interpreting *tim-1* meiotic defects. Each *C. elegans* gonad arm contains hundreds of syncytial germline nuclei arranged along the distal–proximal axis in a spatial progression that follows the temporal progression into and through meiotic prophase (Fig. 3a)[16]. Nuclei entering meiotic prophase undergo a marked spatial reorganization that partitions chromosomes and nucleoli to opposite sides (Fig. 3a, c)[17]. In this 'transition zone', the equivalent of leptotene/zygotene, the chromatin has a crescent-shaped appearance, and homologues initiate pairing[18] by a process that is independent of mature synaptonemal complex (SC)[7,19], an ordered protein structure that holds homologues together. By pachytene, homologous chromosomes redistribute about the nuclear periphery and achieve full alignment and synapsis by means of SC-dependent processes[18,19]. The synapsed homologues (Fig. 3a–c)[17] are proficient in crossover recombination and appear as closely aligned, parallel tracks that stain with 4,6-iamidino-2-phenylindole (DAPI) (Fig. 3b) and have a single 5S rDNA FISH signal (Fig. 3e, f). Chromosomes become desynapsed in diplotene/diakinesis owing to disassembly of the SC. During diakinesis, the homologues are held together by transient physical linkages (chiasmata), the result of crossover recombination and chromosome cohesion distal to the crossover. Wild-type homologues form six axially oriented bivalents.

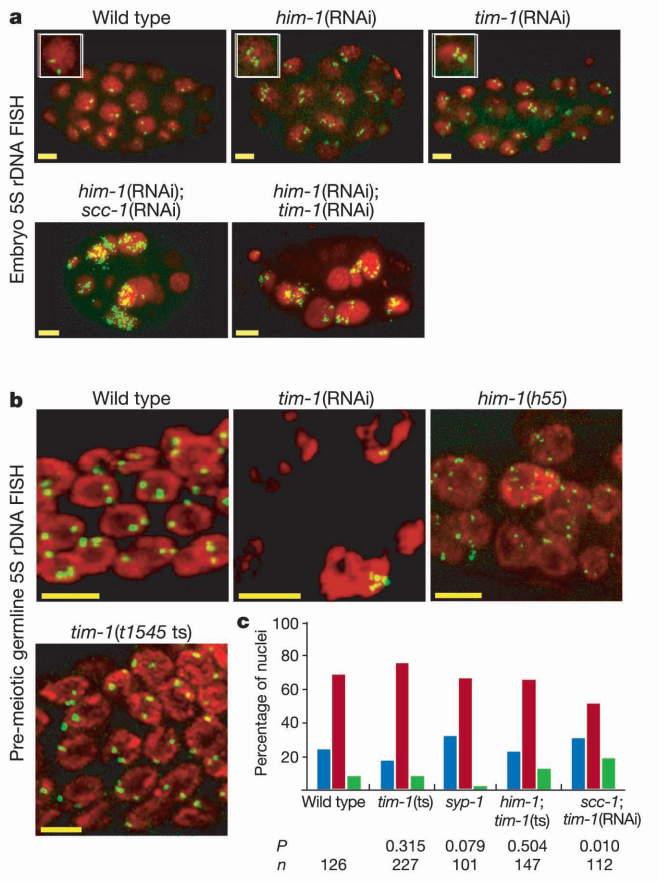

Figure 2 TIM-1, like cohesin subunits, is essential for mitotic chromosome segregation in somatic and germline tissues. **a**, The DNA ploidy of untreated and RNAi-treated embryos was assayed by FISH to 5S rDNA: red, DNA; green, FISH fluorescence. Single RNAi treatment targeting either *tim-1* or *him-1* caused occasional nuclei with more than two FISH signals but most nuclei of dying embryos appeared wild-type, having at most two signals (upper panels). In contrast, severe aneuploidy resulted from double RNAi treatments targeting *him-1* and either *scc-1* or *tim-1* (lower panels). **b**, In pre-meiotic nuclei, *tim-1*(RNAi) and *him-1* null mutations caused aneuploidy, as assayed by FISH. In contrast, pre-meiotic nuclei from *tim-1(t1545*ts*)* and wild-type animals grown at 25 °C were indistinguishable (**b**, **c**). Scale bars, 5 μm. **c**, Graph showing the distribution of FISH signals in pre-meiotic nuclei of different genotypes: blue, one signal; red, two signals; green, more than two signals. *n* is the total number of nuclei scored; *P* is calculated relative to wild type.

We used the *tim-1(t1545*ts*)* allele to assess TIM-1 function in meiotic chromosome cohesion, because it selectively disrupts meiosis but not germline mitosis under a specific temperature-shift regime (Fig. 2b, c, and Methods). Thus, the meiotic defects in *tim-1*(ts) nuclei cannot be attributed to defective germline mitosis.

Imaging of DAPI-stained *tim-1*(ts) mutant nuclei revealed meiotic defects that resembled those caused by RNAi depletion of REC-8, a meiosis-specific cohesin subunit that replaces the mitosis-specific SCC-1 subunit[7]. Transition-zone nuclei of *tim-1*(ts) or *rec-8*(RNAi) mutants had normal polarized organization (Fig. 3c), and a similar proportion of paired and unpaired homologues to that in wild-type nuclei, on the basis of 5S rDNA FISH signals (Fig. 3j and ref. 7). However, both *tim-1*(ts) and *rec-8*(RNAi) mutants had an extended transition zone (Fig. 3c) in which polarized nuclei persisted into the

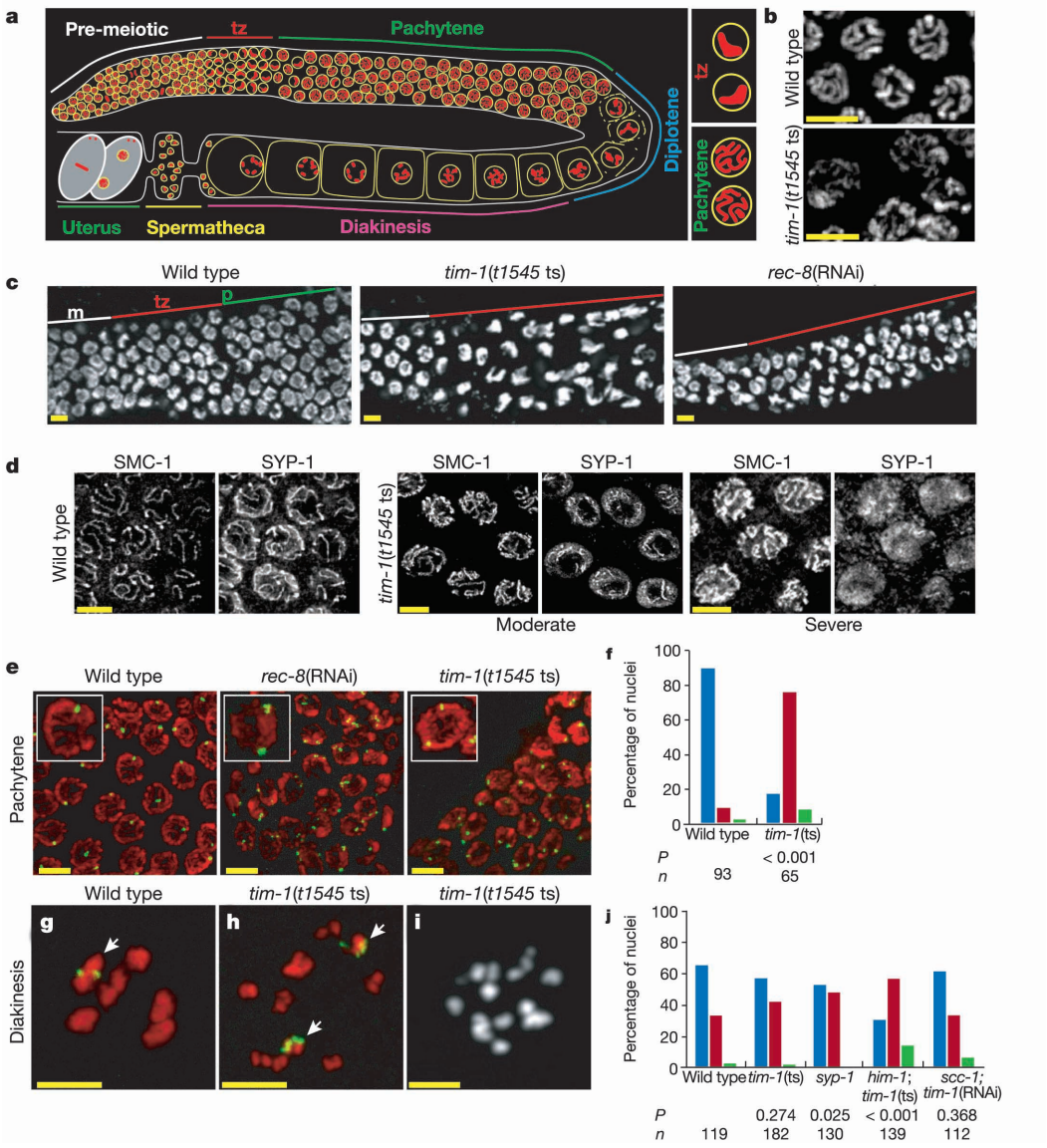

Figure 3 *tim-1* mutants are defective in meiotic chromosome cohesion. **a**, Schematic drawing of an adult hermaphrodite gonad arm: pre-meiotic region (mitotic germ cell proliferation and pre-meiotic DNA replication), transition zone (tz; homologue pairing and initiation of synapsis), pachytene (completion of synapsis and crossover recombination), diplotene (SC disassembly) and diakinesis (homologue association maintained by chiasmata and chromosome cohesion). **b**, Pachytene chromosomes in *tim-1(t1545*ts*)* mutants fail to achieve lengthways alignment typical of synapsed wild-type pachytene chromosomes and appear as single, rather than parallel, DAPI-stained tracks. **c**, DAPI-stained image of a wild-type gonad shows the normal progression of nuclei from mitosis (m), through two stages of meiotic prophase, the transition zone (also known as leptotene/zygotene) and pachytene (p). *tim-1*(ts) and *rec-8*(RNAi) mutants exhibit normal nuclear reorganization and homologue pairing in the transition zone, but the redistribution of the chromosomes toward the nuclear periphery that normally accompanies the onset of pachytene is delayed, causing an extended transition zone. **d**, In *tim-1*(ts) gonads, SC central region component SYP-1 (ref. 19) is localized to short discontinuous patches rather than along the entirety of homologous chromosomes, consistent with a defect in SC assembly. The co-staining marker SMC-1 is unaffected by the *tim-1* mutation. **e**, The two 5S rDNA FISH signals in *tim-1*(ts) pachytene-region nuclei reveal asynapsis of chromosome V homologues. **f**, Quantification of **e** for late-pachytene nuclei: blue, one FISH signal per nucleus; red, two signals; green, more than two signals. **g**, In a wild-type diakinesis nucleus, chromosome V homologues are physically linked in a bivalent (white arrow). **h**, In the *tim-1*(ts) mutant nuclei, chromosome V homologues are prematurely separated (white arrows). **i**, Evidence for sister chromatid separation: more than 12 DAPI-stained bodies are apparent. Scale bars, 5 μm. **j**, Quantification of pairing of transition-zone nuclei. *him-1*(RNAi);*tim-1*(ts) mutants showed significantly decreased pairing of the 5S rDNA locus in transition-zone nuclei compared with wild-type or *syp-1(me17)* mutant animals (see also Supplementary Table 3), indicating that synapsis-independent homologue pairing requires cohesin. Most pre-meiotic nuclei in all three sets of animals had the expected number of FISH signals (one or two), indicating few, if any, mitotic chromosome abnormalities. In contrast, double RNAi of *scc-1* and *tim-1* had negligible effects on pairing of the 5S rDNA locus in transition-zone nuclei, despite its disruption to the pre-meiotic germline (Fig. 2c).

region of the gonad that is normally filled with pachytene nuclei. We reasoned that the extended transition zone might result from disrupted SC assembly due to defective cohesin function. Rec8 is required for the normal formation of the yeast SC[20], and disruption of the *C. elegans* SC by depleting the SC central-region component SYP-1 causes an extended transition zone[19]. Indeed, SYP-1 localization was aberrant (Fig. 3d) in *tim-1*(ts) mutants. SYP-1 assembled in short discontinuous patches along chromosomes of most *tim-1*(ts) pachytene-region nuclei (85%, $n = 62$), rather than continuously along homologous chromosomes, as in wild-type nuclei. In contrast, the co-staining control marker SMC-1 localized properly. The degree of SYP-1 disruption was directly correlated with the severity of the extended transition zone (Fig. 3d). These results provide functional evidence for the involvement of TIM-1 in SC formation, perhaps through its effect on cohesin function.

Although meiotic chromosomes of *tim-1*(ts) or *rec-8*(RNAi) mutants reorganized into a pachytene-like arrangement just before diplotene (Fig. 3b, c), like those of *syp-1* mutants, they failed to achieve the normal lengthwise alignment typical of synapsed pachytene chromosomes (Fig. 3b). Only 17% ($n = 65$) of *tim-1*(ts) nuclei within the late pachytene region had one 5S rDNA FISH signal, in comparison with 89% ($n = 93$) of wild-type nuclei, indicating a severe defect in synapsis (Fig. 3e, f), an outcome expected from aberrant chromosome cohesion.

Homologous chromosomes of *tim-1*(ts) mutants rarely formed chiasmata. Of 142 diakinesis nuclei from wild-type germlines (Fig. 3g), all had six bivalents. Instead, 101 of 105 *tim-1*(ts) nuclei had 7–12 staining bodies, with an average of 10; they were mostly univalents and an occasional bivalent, indicating disrupted homologue linkage (Fig. 3h). Three nuclei had more than 12 bodies (Fig. 3i), implying both homologue and sister chromatid separation, consistent with a disruption of meiotic chromosome cohesion. *rec-8*(RNAi) (ref. 7, data not shown) and *him-1*(ts) (Supplementary Fig. 1d) produced similar results. The partial separation of *tim-1*(ts) sister chromatids probably reflects the incomplete disruption of TIM-1 activity by the temperature-sensitive mutation. Together, the meiotic defects caused by the disruption of *tim-1*—the extended transition zone correlated with mislocalized SYP-1, asynapsis in pachytene, and the lack of chiasmata in diakinesis—mimic the defects caused by a disruption of meiotic cohesin, providing compelling evidence for the essential role of *tim-1* in meiotic chromosome cohesion.

TIM-1 could act directly with cohesin throughout meiotic prophase to promote chromosome cohesion, or it could facilitate cohesin stability or localization to chromatin, acting only before meiotic prophase. To evaluate these models, we first defined the *C. elegans* meiotic cohesin subunits and compared their germline localization with that of TIM-1. In many organisms, meiosis-specific cohesin subunits replace their mitotic paralogues[15]. Although the *C. elegans* REC-8 protein substitutes for its mitotic SCC-1 paralogue[7], the other mitotic cohesin subunits have no worm paralogues, making their replacement in meiosis unlikely.

Consistent with this premise is the observation that SMC-1, SMC-3 and SCC-3 recapitulate the meiotic localization pattern of REC-8. All four proteins associate with the chromatin of transition-zone nuclei (Fig. 4a, b, and data not shown), which is consistent with the loading of meiotic cohesin before or during pre-meiotic S phase. SMC-1 co-localizes with REC-8 in pachytene nuclei, and all four proteins assemble along the longitudinal axes of synapsed chromosomes (Fig. 4c). Moreover, two findings show that SMC-1 localization to pachytene chromosomes does not require chromosomes to have a pairing partner and SC. In XO males, SMC-1 antibody staining is evident along the unpaired X chromosome (Fig. 4d). In XO males carrying a IV:X fusion chromosome (*mnT12*), in which IV is paired and X is unpaired, SMC-1 localizes along the entirety of the fusion chromosome (Fig. 4d). Finally, SMC-1 co-localizes with REC-8 in diakinesis, and SMC-1, SMC-3 and REC-8 all adopt a cruciform pattern (Fig. 4e), which is consistent with a role for these proteins in maintaining connections between homologues and between sister chromatids. In contrast, SCC-3 localized throughout the chromatin, indicating a possible additional role for SCC-3 in diakinesis not played by other cohesins (Fig. 4f).

TIM-1 protein localization differed remarkably from that of meiotic cohesin, suggesting that TIM-1 facilitates the loading or stability of cohesin proteins, rather than serving as an integral complex component. TIM-1 was diffusely distributed throughout pre-meiotic nuclei and disappeared abruptly as nuclei entered meiotic prophase (Fig. 4a, b). Unlike cohesin subunits, TIM-1 was not detected in transition-zone or pachytene nuclei, but reappeared in diplotene and accumulated in diakinesis. TIM-1 was excluded from chromosomes in diakinesis and probably accumulates in oocytes only for its subsequent function in embryonic mitosis (Fig. 4g).

To determine whether TIM-1 affects cohesin subunits, we examined the distribution of REC-8, SCC-3, SMC-1 and SMC-3 in *tim-1* mutants. REC-8 was not detectable on *tim-1*(ts) (Fig. 5a–c) or *tim-1*(RNAi) chromosomes (data not shown) in meiotic prophase, although it was present in pre-meiotic nuclei (Fig. 5a), indicating that TIM-1 affects the stability or loading of REC-8 but not its production. REC-8 depletion did not alter TIM-1 localization in pre-meiotic nuclei (data not shown), which is consistent with TIM-1's regulating REC-8. In *tim-1* mutants, SCC-3 concentrations were variably reduced, and in half the gonads the residual protein was undetectable on the meiotic chromosomes (Fig. 5a–c). In contrast, SMC-1 seemed properly localized to meiotic chromosomes of *tim-1*(ts) (Fig. 5a–c) or *tim-1*(RNAi) mutant gonads (data not shown), suggesting that a loss of TIM-1 function does not affect SMC localization. TIM-1 therefore differs from the yeast Scc2/4 cohesin regulatory proteins, which affect the loading of both SMC and non-SMC cohesin components[21], and differs from yeast Pds5, which persists with the cohesin complex[22,23].

If SMC-1 and SMC-3 load onto chromatin independently of non-SMC proteins, as suggested by our data, then disruption of REC-8 should not affect SMC protein localization. Indeed, severe depletion of *rec-8* by RNAi (Fig. 1h) caused no detectable change in SMC-1 or SMC-3 localization but did cause mislocalization of SCC-3 (Fig. 5d, e, and Supplementary Fig. 1e). SCC-3 mislocalization is consistent with structural studies in budding yeast showing that Scc1 mediates the interaction between Scc3 and the Smc1/Smc3 heterodimer[24]. Furthermore, SMC-1 and SMC-3 localization seemed unperturbed under more stringent conditions in which *rec-8*(RNAi) treatment was performed in *tim-1*(ts) mutants (Fig. 5f). These results indicate that TIM-1 promotes meiotic chromosome cohesion through its regulation of cohesin subunits and that TIM-1 might preferentially regulate the loading or stability of REC-8 and SCC-3 before leptotene/zygotene. These results also show the differential loading or retention of individual cohesin subunits at the onset of meiosis.

The presence of SMC proteins on *tim-1*(ts); *rec-8*(RNAi) mutant chromosomes raised the possibility that cohesion activity might persist, thus obscuring the complete role of cohesin in meiosis. Reducing SMC-1 concentrations with RNAi in a *tim-1*(ts) mutant revealed the involvement of cohesin in the early pairing of homologues before synapsis. Although the chromosomes of *him-1*(RNAi);*tim-1*(ts) animals underwent the initial spatial reorganization typical during leptotene/zygotene, only 30% of chromosome V homologues paired at the 5S rDNA locus in comparison with 65% in untreated animals, reflecting a 54% decrease in pairing (Fig. 3j, Supplementary Table 3).

This defect in early pairing is unlikely to be a reflection of aberrant germline mitosis, because the pre-meiotic regions of *him-1*(RNAi);*tim-1*(ts) and wild-type animals were indistinguishable by FISH analysis (Fig. 2c, and Supplementary Table 3).

Moreover, the simultaneous disruption of *tim-1* and the mitotic cohesin gene *scc-1* by RNAi failed to disrupt pairing at the 5S rDNA locus (Fig. 3j, and Supplementary Table 3), although it did disrupt germline mitosis (Fig. 2c).

The defect in pairing cannot be attributed to the disruption of SYP-1 and hence the SC, because pairing at the 5S rDNA locus was more severely disrupted in *him-1*(RNAi);*tim-1*(ts) mutants than in *syp-1* mutants (30% versus 52%, a 42% decrease in pairing; Fig. 3j, and Supplementary Table 3). These results show that synapsis-independent homologue pairing relies in part on cohesin function, thus revealing a crucial role for cohesin not previously demonstrated in metazoans. These experiments probably underestimate the contribution of cohesin to pairing, because efforts to minimize defects in pre-meiotic chromosome segregation required that cohesin function be disrupted only partly.

Our work has revealed unexpected roles in chromosome segregation for the *C. elegans* homologue of the *Drosophila timeless* gene, a key regulator of circadian rhythm. *C. elegans* TIM-1 interacts

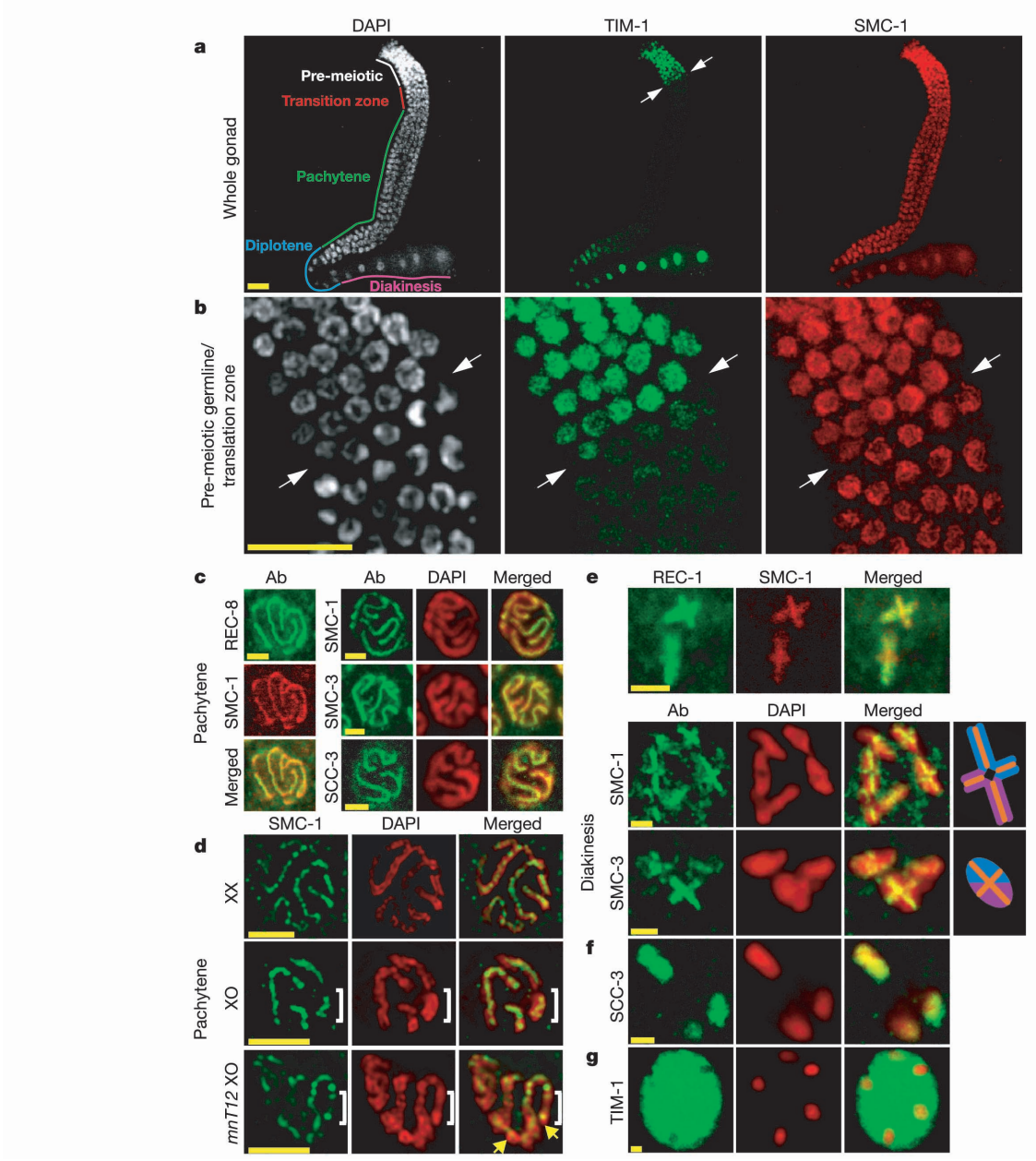

Figure 4 TIM-1 is restricted to pre-meiotic nuclei, unlike meiotic cohesin, which localizes between sister chromatids throughout meiotic prophase. **a**, **b**, Antibody and DAPI fluorescence images of dissected wild-type gonads. Intense nuclear TIM-1 accumulation observed in pre-meiotic nuclei was reduced abruptly as nuclei entered meiosis. The boundary between the pre-meiotic region and the transition zone (opposing white arrows) is characterized by crescent-shaped chromatin (**b**). **c**, SMC-1, SMC-3 and SCC-3 proteins co-localize with REC-8 along the length of pachytene chromosomes. **d**, Anti-SMC antibody staining along the unpaired male X chromosome (dense DAPI staining, white brackets) of wild-type XO males and those with the *mnT12(IV;X)* fusion chromosome shows that SMC-1 localization is not dependent on homologous chromosome pairing and SC formation. *mnT12* chromosome ends are marked by yellow arrows. **e**, SMC-1, SMC-3 and REC-8 have identical cruciform staining patterns, consistent with their function in the meiotic cohesin complex. At the right is a diagram of the cohesin staining pattern in early and late diakinesis bivalents showing cohesin (orange) and sister chromatid pairs (blue and purple). **f**, SCC-3 localizes to the interface of sister chromatids and homologous chromosomes and also throughout the bivalent, indicative of additional functions. **g**, By diakinesis, maternally loaded TIM-1 fills the nucleoplasm but is excluded from DNA. Scale bars, 20 μm (**a**, **b**); 2 μm (**c**–**g**).

physically with the cohesin complex and thereby mediates chromosome cohesion. Not only is TIM-1 critical for mitotic chromosome segregation in somatic and germline tissues, it is also essential for chromosome segregation in meiosis. Through its crucial role in localizing non-SMC cohesin subunits to chromatin, before or during the pre-meiotic S phase, TIM-1 has a fundamental role in meiosis, stabilizing homologous chromosome associations during synapsis and sister chromatid cohesion in diplotene/diakinesis. This differential effect of TIM-1 on the non-SMC subunits suggests the independent loading or stabilization of cohesin components and indicates that SMC proteins might retain partial function without the context of the entire cohesin complex.

Given the vital role of *C. elegans tim-1* in chromosome cohesion and the essential function of mouse *mTim1* in embryo viability, we suggest that the evolution of the involvement of *timeless* in the *Drosophila* circadian rhythm resulted from a duplication and subsequent specialization of the fly *timeout* gene, which more closely resembles the single paralogue present in *C. elegans*, mice and humans. Comparison of predicted protein structures reinforces this view. *Drosophila* TIMEOUT, *C. elegans* TIM-1 and mouse mTim1 all have contiguous HEAT/Armadillo (Arm) repeats that reside within a similar region of each protein (Supplementary Fig. 2). In contrast, the HEAT/Arm repeats of *Drosophila* TIMELESS are interrupted by one of two PERIOD-interaction domains[25], indicating that this change could enhance the association between PERIOD and TIMELESS. Given the unique structure of *Drosophila* TIMELESS and the conclusions of our present study, we propose that chromosome cohesion, rather than circadian rhythm regulation, is the ancient and conserved function for *timeless* paralogues in metazoans. □

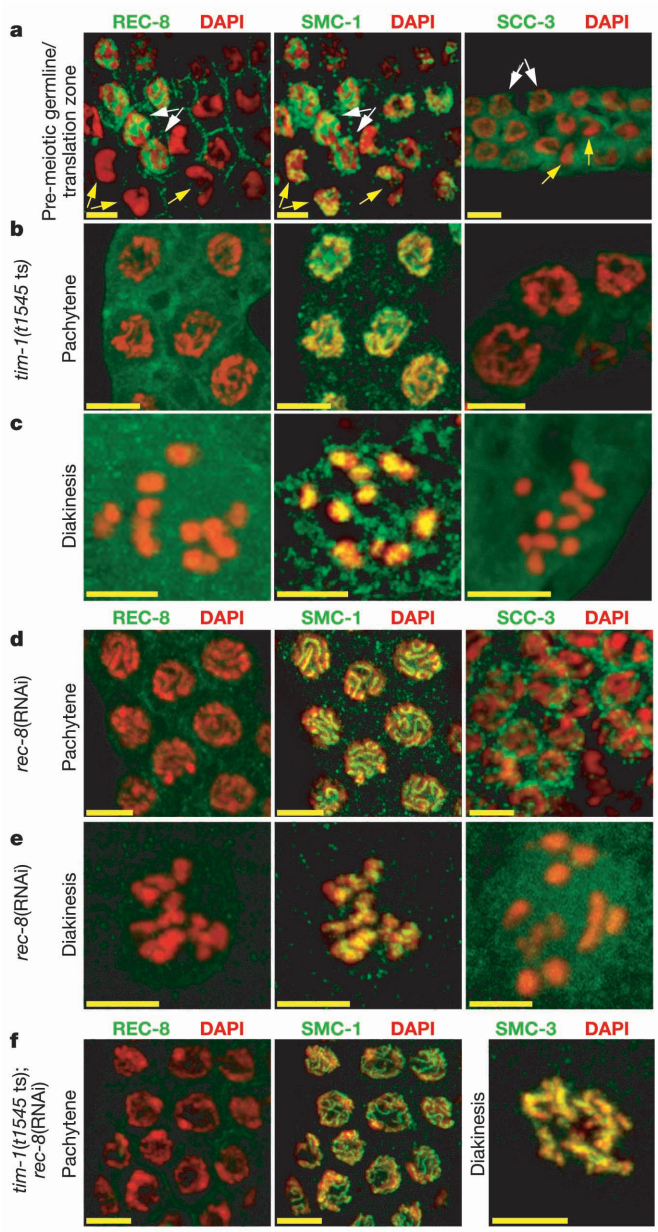

Figure 5 Loss of *tim-1* function preferentially disrupts the loading or stability of non-SMC cohesin subunits. Immunofluorescence photomicrographs of cohesin subunits in *tim-1*(ts) (**a**–**c**), *rec-8*(RNAi) (**d**, **e**) and *tim-1*(ts);*rec-8*(RNAi) (**f**) mutant germlines. **a**, accumulation of SMC-1, REC-8 and SCC-3 is unperturbed in pre-meiotic nuclei (white arrowheads) of *tim-1*(ts) mutants. However, on transition-zone chromatin (yellow arrowheads) of *tim-1*(ts) mutants, REC-8 staining is undetectable and SCC-3 staining is severely reduced, but SMC-1 staining is normal (also Fig. 3d). **b**, **c**, Similarly, REC-8 and SCC-3 staining is severely disrupted in pachytene (**b**) and diakinesis (**c**) chromosomes of *tim-1*(ts) mutants, but SMC-1 staining is normal. **d**, **e**, Unlike SCC-3 staining, SMC-1 staining (and SMC-3; Supplementary Fig. 1e) on pachytene (**d**) and diakinesis (**e**) chromosomes is unaffected by *rec-8*(RNAi), showing the stable chromatin association of cohesin SMC subunits with few or no non-SMC components (see Fig. 1h for quantification of the REC-8 depletion). **f**, In *tim-1*(ts);*rec-8*(RNAi) double mutants, SMC-1 and SMC-3 localize to chromosomes in pachytene (see also Supplementary Fig. 1e) and diakinesis. Note that diakinesis chromosomes often fail to resolve in the double mutants. Scale bars, 5 μm.

Methods

him-1 encodes SMC-1

Deletion mapping of the SMC-1 ORF F28B3.7 by polymerase chain reaction (PCR) placed the gene under deletion *sDf4* but not *hDf6*, in an interval harbouring five genes with lethal null phenotypes, including the likeliest candidate *him-1*. The temperature-sensitive *him-1(e879)* allele and two genetic *him-1* null alleles, *h55* and *h134*, have been described previously[5,26]. A 9.3-kilobase (kb) genomic PCR product covering F28B3.7 rescued the sterility of *him-1(h55)* mutants, and DNA sequence changes were identified for all three *him-1* alleles, indicating that *him-1* encodes the Smc1 homologue. The *him-1(h55)* null allele carries a deletion that removes portions of the second exon and intron. The deletion is predicted to disrupt the splicing of the second and third exons and probably causes a frame shift that aborts translation after amino acid 250. The *him-1(h134)* null allele causes a C–T transition at nucleotide 3271 of the coding sequence. This mutation generates a premature stop codon predicted to truncate 172 amino acids from the carboxy terminus. The *him-1(e879)* partial loss-of-function allele results in the P1138S substitution. cDNA sequencing of *him-1* agrees with the predicted intron–exon boundaries for F28B3.7 (GenBank accession no. 17506950) with the exception of intron 7, where the actual 3′ splice site is 57 nucleotides downstream of the predicted 3′ splice site.

Antibody production

The following antigens were used to generate antibodies: C-terminal peptides to DPY-27, MIX-1, SMC-3 and TIM-1; amino-terminal peptide to SCC-3; SMC-1 residues 652–1075 fused to a His_6 tag; SCC-1 residues 207–500 and TIM-1 residues 286–1001 fused to glutathione *S* transferase tags. TIM-1 peptide antibodies recognize a protein of M_r 150K from wild-type extracts but no protein from extracts of animals treated with RNAi against *tim-1* (Fig. 1d), thus establishing antibody specificity. The antibodies also detected a *tim-1* RNAi-sensitive product of M_r 120K (Fig. 1d), which seems to be a TIM-1 post-lysis cleavage product, consistent with (1) the single 5.5-kb *tim-1* transcript identified on northern blots (Fig. 1g) and (2) the DNA sequence of *tim-1* cDNA and products from PCR with reverse transcription. Immunofluorescence staining was imaged by confocal microscopy[27]. Chromosomes in Fig. 4d were imaged on an API DeltaVision deconvolution microscope system.

Worm lysates, embryonic extracts and immunoprecipitation

Whole worm lysates were prepared from at least 30 animals washed with PBS and boiled in SDS sample buffer with 3 M urea. Embryo extract preparation and immunoprecipitation were performed as described[28].

Genetics

Gene function was disrupted by injecting double-stranded RNA into wild-type (N2), *unc-32(e189) tim-1(t1545*ts*)/qC1 [dpy-19(e1259) glp-1(q339)] III* or *unc-32(e189) tim-1(t1545)/hT2 III* strains. *tim-1(t1545*ts*)* homozygotes are maternal-effect lethal at both 20 and 25 °C (ref. 29), and maternally rescued animals (m^+/z^-) exhibit meiotic defects when grown at 25 °C. For analysis of *tim-1(t1545*ts*)* meiotic phenotypes, embryos were collected at 20 °C from *tim-1* heterozygotes and allowed to develop into adults at 25 °C; maternally rescued (m^+/z^-) *tim-1* homozygotes were isolated by picking Unc hermaphrodites. The allele *t1545* was originally described as a maternal-effect lethal mutation in the gene *csg-5* (ref. 29). It was subsequently shown to be a temperature-sensitive *tim-1* allele (M.J. and A.E.R., unpublished observations).

mnT12(IV;X)/+ males were generated by crossing homozygous *mnT12* hermaphrodites with wild-type males.

Double-stranded RNA interference

Templates for *him-1*, *scc-1*, *scc-3*, *rec-8* and *tim-1* RNA transcription were generated by PCR amplification from N2 genomic DNA with the use of the primer sets listed in Supplementary Table 4. The *smc-3* template was amplified by PCR using T3 and T7 primers from the Kohara cDNA *yk361c10*. Double-stranded RNA (1–5 mg ml^{-1}) was injected into the gonads of young gravid hermaphrodites.

For immunostaining and FISH studies the following RNAi-treated animals were scored: (1) *rec-8*(RNAi), F_1 progeny from injected animals; (2) *scc-1*(RNAi);*tim-1*(RNAi) or *him-1*(RNAi);*tim-1*(RNAi), injected parents dissected 48 h after injection; (3) *him-1*(RNAi);*tim-1*(ts), injected *tim-1*(ts) adults (grown at 25 °C as above) dissected 24 h after injection; (4) *him-1*(RNAi), *tim-1*(RNAi), *him-1*(RNAi);*scc-1*(RNAi) and *him-1*(RNAi);*tim-1*(RNAi), injected parents dissected 24 h after injection. FISH analysis was performed on embryos dissected from adults 48 h after injection with double-stranded RNA from the targeted gene(s).

FISH and statistical analysis

FISH with 5S rDNA was performed as described[27]. The number of FISH signals per nucleus was counted for the mitotic region (50 μm or less from the distal tip), transition zone (30 μm or less from the first appearance of crescent-shaped DAPI figures) and pachytene (40 μm or less distal to diplotene). The nuclei were distributed into five categories: one, two, three, four and more than four FISH signals per nucleus. The statistical comparisons of FISH signals in mutant and wild-type nuclei were performed on the categories of one, two and more than two FISH signals per nucleus by pairwise χ^2 tests. For the transition-zone nuclei analysed in Fig. 3j, the distribution of FISH signals in the population of nuclei for each genotype reflected the distribution of FISH signals in each individual animal scored.

Received 10 March; accepted 1 May 2003; doi:10.1038/nature01697.

1. Hirano, T. Chromosome cohesion, condensation, and separation. *Annu. Rev. Biochem.* **69,** 115–144 (2000).
2. Nasmyth, K. Disseminating the genome: joining, resolving, and separating sister chromatids during mitosis and meiosis. *Annu. Rev. Genet.* **35,** 673–745 (2001).
3. Sumara, I. *et al.* The dissociation of cohesin from chromosomes in prophase is regulated by Polo-like kinase. *Mol. Cell* **9,** 515–525 (2002).
4. Uhlmann, F., Lottspeich, F. & Nasmyth, K. Sister-chromatid separation at anaphase onset is promoted by cleavage of the cohesin subunit Scc1. *Nature* **400,** 37–47 (1999).
5. Hodgkin, J., Horvitz, H. R. & Brenner, S. Nondisjunction mutants of the nematode *Caenorhabditis elegans*. *Genetics* **91,** 67–94 (1979).
6. Broverman, S. A. & Meneely, P. M. Meiotic mutants that cause a polar decrease in recombination on the X chromosome in *Caenorhabditis elegans*. *Genetics* **136,** 119–127 (1994).
7. Pasierbek, P. *et al.* A *Caenorhabditis elegans* cohesion protein with functions in meiotic chromosome pairing and disjunction. *Genes Dev.* **15,** 1349–1360 (2001).
8. Chuang, P. T., Albertson, D. G. & Meyer, B. J. DPY-27: A chromosome condensation protein homolog that regulates *C. elegans* dosage compensation through association with the X chromosome. *Cell* **79,** 459–474 (1994).
9. Lieb, J. D., Albrecht, M. R., Chuang, P. T. & Meyer, B. J. MIX-1: An essential component of the *C. elegans* mitotic machinery executes X chromosome dosage compensation. *Cell* **92,** 265–277 (1998).
10. Jeon, M., Gardner, H. F., Miller, E. A., Deshler, J. & Rougvie, A. E. Similarity of the *C. elegans* developmental timing protein LIN-42 to circadian rhythm proteins. *Science* **286,** 1141–1146 (1999).
11. Williams, J. A. & Sehgal, A. Molecular components of the circadian system in *Drosophila*. *Annu. Rev. Physiol.* **63,** 729–755 (2001).
12. Young, M. W. & Kay, S. A. Time zones: A comparative genetics of circadian clocks. *Nature Rev. Genet.* **2,** 702–715 (2001).
13. Benna, C. *et al.* A second timeless gene in *Drosophila* shares greater sequence similarity with mammalian tim. *Curr. Biol.* **10,** R512–R513 (2000).
14. Gotter, A. L. *et al.* A time-less function for mouse timeless. *Nature Neurosci.* **3,** 755–756 (2000).
15. Petronczki, M., Siomos, M. F. & Nasmyth, K. Un ménage à quatre: the molecular biology of chromosome segregation in meiosis. *Cell* **112,** 423–440 (2003).
16. Schedl, T. in *C. elegans II* (eds Riddle, D. L., Blumenthal, T., Meyer, B. J. & Priess, J. R.) 241–270 (Cold Spring Harbor Laboratory Press, Cold Spring Harbor, New York, 1997).
17. MacQueen, A. J. & Villeneuve, A. M. Nuclear reorganization and homologous chromosome pairing during meiotic prophase require *C. elegans chk-2*. *Genes Dev.* **15,** 1674–1687 (2001).
18. Dernburg, A. F. *et al.* Meiotic recombination in *C. elegans* initiates by a conserved mechanism and is dispensable for homologous chromosome synapsis. *Cell* **94,** 387–398 (1998).
19. MacQueen, A. J., Colaiacovo, M. P., McDonald, K. & Villeneuve, A. M. Synapsis-dependent and -independent mechanisms stabilize homolog pairing during meiotic prophase in *C. elegans*. *Genes Dev.* **16,** 2428–2442 (2002).
20. Klein, F. *et al.* A central role for cohesins in sister chromatid cohesion, formation of axial elements, and recombination during yeast meiosis. *Cell* **98,** 91–103 (1999).
21. Ciosk, R. *et al.* Cohesin's binding to chromosomes depends on a separate complex consisting of Scc2 and Scc4 proteins. *Mol. Cell* **5,** 243–254 (2000).
22. Hartman, T., Stead, K., Koshland, D. & Guacci, V. Pds5p is an essential chromosomal protein required for both sister chromatid cohesion and condensation in *Saccharomyces cerevisiae*. *J. Cell Biol.* **151,** 613–626 (2000).
23. Panizza, S., Tanaka, T., Hochwagen, A., Eisenhaber, F. & Nasmyth, K. Pds5 cooperates with cohesin in maintaining sister chromatid cohesion. *Curr. Biol.* **10,** 1557–1564 (2000).
24. Haering, C. H., Lowe, J., Hochwagen, A. & Nasmyth, K. Molecular architecture of SMC proteins and the yeast cohesin complex. *Mol. Cell* **9,** 773–788 (2002).
25. Vodovar, N., Clayton, J. D., Costa, R., Odell, M. & Kyriacou, C. P. The *Drosophila* clock protein Timeless is a member of the Arm/HEAT family. *Curr. Biol.* **12,** R610–R611 (2002).
26. Howell, A. M., Gilmour, S. G., Mancebo, R. A. & Rose, A. M. Genetic analysis of a large autosomal region in *Caenorhabditis elegans* by the use of a free duplication. *Genet. Res.* **49,** 207–213 (1987).
27. Howe, M., McDonald, K. L., Albertson, D. G. & Meyer, B. J. HIM-10 is required for kinetochore structure and function on *Caenorhabditis elegans* holocentric chromosomes. *J. Cell Biol.* **153,** 1227–1238 (2001).
28. Chu, D. S. *et al.* A molecular link between gene-specific and chromosome-wide transcriptional repression. *Genes Dev.* **16,** 796–805 (2002).
29. Gonczy, P. *et al.* Dissection of cell division processes in the one cell stage *Caenorhabditis elegans* embryo by mutational analysis. *J. Cell Biol.* **144,** 927–946 (1999).

Supplementary Information accompanies the paper on **www.nature.com/nature**.

Acknowledgements We thank D. King for the MALDI–MS analyses, M. Ralston for advice on statistical methods, J. Loidl, A. Villeneuve and Y. Kohara for useful reagents, G. Csankovszki for the RNA blot, M. Colaiacovo and A. Villeneuve for discussions, and T. Cline, A. Severson and C. Tsai for comments on the manuscript. This work was supported by the Leukemia and Lymphoma Society (R.C.C.), the American Cancer Society (D.P.) and the National Institutes of Health (A.E.R.). B.J.M. is an investigator and R.C.C. an associate of the Howard Hughes Medical Institute.

Competing interests statement The authors declare that they have no competing financial interests.

Correspondence and requests for materials should be addressed to B.J.M. (bjmeyer@uclink.berkeley.edu).

Cks1-dependent proteasome recruitment and activation of *CDC20* transcription in budding yeast

May C. Morris*†, Peter Kaiser*†, Stanislav Rudyak*, Chris Baskerville*, Mark H. Watson*† & Steven I. Reed*

** The Scripps Research Institute, Department of Molecular Biology, 10550 North Torrey Pines Road, La Jolla, California 92037, USA*

Cks proteins are small evolutionarily conserved proteins that interact genetically and physically with cyclin-dependent kinases. However, in spite of a large body of genetic, biochemical and structural research, no compelling unifying model of their functions has emerged[1,2]. Here we show, by investigating the essential role of Cks1 in *Saccharomyces cerevisiae*, that the protein is primarily involved in promoting mitosis by modulating the transcriptional activation of the APC/C protein–ubiquitin ligase activator Cdc20. Cks1 is required for both the periodic dissociation of Cdc28 kinase from the *CDC20* promoter and the periodic association of the proteasome with the promoter. We propose that the essential role of Cks1 is to recruit the proteasome to, and/or dissociate the Cdc28 kinase from, the *CDC20* promoter, thus facilitating transcription by remodelling transcriptional complexes or chromatin associated with the *CDC20* gene.

cks1-35 cells arrest in metaphase with high levels of the anaphase inhibitor securin, known as Pds1 in *S. cerevisiae*[3,4]. Mitotic progression of wild-type, unperturbed cells is regulated primarily by the accumulation of mitotic cyclins[5–7] and activation of the protein–ubiquitin ligase APC/C by its substrate-specific activator Cdc20. This enables the proteolysis of Pds1 and the onset of anaphase[8–10]. The isolation of *CDC20* as a strong multicopy suppressor of a *cks1* temperature-sensitive mutant (this study; data not shown)

† Present addresses: Centre de Recherches en Biochimie Macromoléculaire—CNRS-UPR1086, 1919 Route de Mende, 34293 Montpellier, France (M.C.M.); University of California Irvine, Department of Biological Chemistry, Irvine, California 92697-1700, USA (P.K.); Gemin X Biotechnologies Inc., CP/PO Box 477, Place du Parc, Montreal, Quebec, Canada H2W 2M9 (M.H.W.).